symmetry

MDPI

Article

Unveiling Risk Reconfiguration in Freeway Merging Areas: A Spatiotemporal Framework for Conflict Prediction and Hotspot Migration in CAV Mixed Traffic

Qiang Luo [1], Lili Yang [1], Yanni Ju [2,3,*], Gen Li [4], Xiangyan Guo [1] and Xinqiang Chen [5]

[1] School of Civil Engineering and Transportation, Guangzhou University, Guangzhou 510006, China
[2] Department of Road Traffic Management, Sichuan Police College, Luzhou 646000, China
[3] Intelligent Policing Key Laboratory of Sichuan Province, Luzhou 646000, China
[4] College of Automobile and Traffic Engineering, Nanjing Forestry University, Nanjing 210037, China
[5] Institute of Logistics Science and Engineering, Shanghai Maritime University, Shanghai 201306, China
* Correspondence: yanniju@scpolicec.edu.cn

Abstract

The transition to mixed traffic flows comprising Connected and Automated Vehicles (CAVs) and Human-Driven Vehicles (HVs) induces a fundamental spatial reconfiguration of risk in freeway merging areas. This study proposes a novel spatiotemporal safety assessment framework to characterize the dynamic evolution of risk hotspots. Unlike traditional models, the framework integrates a conflict prediction model based on Negative Binomial regression with a high-resolution, grid-based risk mapping technique. By applying this framework to data from a microscopically simulated and carefully calibrated environment, we successfully identify a distinct migration pattern of risk hotspots: as CAV penetration increases, high-risk zones shift from the static geometric bottleneck at the ramp merge point to a dynamic interaction interface on the mainline. This paradigm shift is further quantified using a multi-dimensional indicator system. A case study demonstrates that increasing the CAV penetration rate from 10% to 50% can improve the safety grade of a merging area from D (Poor) to A (Excellent). The proposed framework provides a practical tool for refined safety diagnostics and offers insights for spatiotemporal risk analysis, informing the development of future cooperative control strategies in mixed traffic environments.

Keywords: traffic safety; freeway merging area; mixed traffic flow; traffic conflict prediction; spatiotemporal safety assessment; risk distribution modeling

Check for updates

Academic Editor: Chengxi Zhang

Received: 18 April 2026
Revised: 9 May 2026
Accepted: 9 May 2026
Published: 12 May 2026

Copyright: © 2026 by the authors. Licensee MDPI, Basel, Switzerland. This article is an open access article distributed under the terms and conditions of the Creative Commons Attribution (CC BY) license.

1. Introduction

The merging area of urban expressways serves as a critical point where traffic flows converge, exhibiting a significantly higher accident risk compared to basic segments, and its safety performance substantially impacts the stable operation of the entire road network [1–3]. With the rapid advancement of Connected and Automated Vehicles (CAVs), mixed traffic flows comprising CAVs and human-driven vehicles represent an inevitable transitional stage in the evolution of Intelligent Transportation Systems. This mixed environment not only alters traditional traffic dynamics but also introduces new analytical challenges for safety assessment in merging areas. On the one hand, real-world accident data is extremely scarce during the initial promotion stage of CAVs, rendering post hoc evaluation methods reliant on historical statistics inadequate. On the other hand, the interaction between CAVs and human-driven vehicles generates complex, nonlinear spatiotemporal

risk patterns that are difficult to capture with traditional macroscopic safety metrics. Consequently, there is an urgent need to develop a new safety assessment framework that integrates proactive prediction with spatiotemporally refined analysis. By establishing predictive mathematical models (e.g., for conflict frequency) and applying associated optimization methods (e.g., for parameter calibration and control strategy design), this framework can systematically address the safety challenges of merging areas under mixed traffic flows. It thereby provides theoretical support for proactive safety management and transportation system optimization.

Research on the impact of mixed traffic flows comprising CAVs and human-driven vehicles (HVs) has delineated a clear framework, spanning from macroscopic performance to microscopic mechanisms. Macroscopic simulation studies indicate that the introduction of CAVs can effectively enhance road capacity, improve traffic flow stability, and reduce emissions [4,5]. At the microscopic safety level, CAVs demonstrate significant safety advantages in routine driving as well as interaction scenarios such as merging and lane-changing, particularly in adverse conditions where they effectively reduce conflicts and delays [6,7]. Their safety benefits are generally positively correlated with penetration rates, leading to systemic improvements once a certain threshold (e.g., 25–30%) is reached [8,9]. From a theoretical perspective, research employing methods such as fundamental diagram models and evolutionary game theory has provided in-depth insights into the heterogeneous interaction processes between CAVs and HVs in behaviors like car-following and lane-changing, as well as their impact on the stability of mixed traffic flows [10–12]. Recently, the analysis of traffic conflict hotspots has begun to leverage CAV data to delineate risk contours in mixed traffic streams, evaluating the safety implications of connectivity technologies [13]. These findings lay an important foundation for understanding the potential benefits of CAV-integrated mixed traffic. However, existing studies have predominantly focused on CAV performance per se or the macroscopic efficiency of mixed traffic, with few systematically addressing the new risk assessment challenges arising from heterogeneous vehicle interactions from a methodological perspective of safety evaluation. During the transitional phase of mixed traffic, where accident data remain scarce, there is a pressing need to develop proactive safety assessment methods based on real-time interaction behaviors, with the Traffic Conflict Technique (TCT) being a prime example.

The TCT, as a non-accident proactive safety analysis method, assesses risk by quantifying interaction behaviors among road users, effectively compensating for the insufficiency of historical accident data. The development of TCT has evolved through stages of methodological construction, technological integration, and scenario expansion. During the methodological construction phase, research focused on standardizing and refining conflict indicators (e.g., Pseudo Time-to-Collision, PTTC [14]) and establishing a conflict severity grading system [15], laying the foundation for reliable application of TCT. With technological advancements, the integration of TCT with methods such as microscopic simulation and extreme value theory has enabled efficient generation of large-scale conflict data and long-term accident risk inference based on small samples, respectively [16,17]. Concurrently, the sub-field of traffic conflict hotspot analysis, which aims to identify and analyze locations with concentrated conflicts, has seen significant methodological evolution. The advent of high-resolution data from unmanned aerial vehicles (UAVs) and drones has enabled the precise identification of microscopic-level hotspots, while spatial statistical methods like Kernel Density Estimation (KDE) have become standard for visualizing risk agglomeration [18–20]. Recent studies have further expanded the temporal dimension, investigating the spatiotemporal evolution of conflicts across different time periods and complex scenarios [21]. This progression has shifted TCT from "phenomenon description" toward "mechanism modeling" and "risk prediction." In terms of application, the scope of

TCT has expanded from traditional intersections to complex environments such as highway merging areas [22,23], heterogeneous traffic flows [24], and intelligent tunnels [25]. Conflict hotspot analysis has similarly diversified, extending to high-risk scenarios like highway merging zones and inclement weather operations [26]. These advancements collectively drive the evolution of TCT from a post hoc analytical tool to a proactive safety management instrument. In particular, the deep integration of TCT with microscopic simulation provides a critical tool for evaluating the safety conditions of emerging traffic environments, such as mixed CAV traffic, under controllable settings.

Merging areas, as bottlenecks where traffic flows inevitably converge, have long been a focal point in safety evaluation research. Given the scarcity of high-quality historical accident data, methods like the Traffic Conflict Technique (TCT) are widely used for safety assessment in these locations. This has spurred multidimensional methodological explorations: studies on control evaluation have quantified the efficacy of measures like ramp metering in reducing conflicts [27]; efforts in comprehensive assessment have developed multi-indicator safety evaluation systems [28,29]; and theoretical applications have introduced new perspectives, such as traffic wave and driver workload theories. Additionally, research has revealed the influence mechanisms of road geometry and traffic flow parameters on conflict formation [30] and extended application scenarios to specific complex environments such as underground interchanges and construction zones [23]. However, most existing studies are based on traditional human-driven traffic environments, and the developed evaluation systems predominantly rely on macroscopic or aggregated conflict indicators (e.g., total conflict frequency within a region or static density maps). Such approaches often standardize conflict thresholds and focus on identifying where risks aggregate, but they struggle to mechanistically explain how heterogeneous interactions dynamically shape the fine-grained, time-varying spatial distribution of conflicts. This makes it difficult to capture the specific spatial distribution and dynamic evolution patterns of risks within merging areas. In a mixed CAV traffic environment, the spatiotemporal characteristics of vehicle interactions may undergo qualitative changes. This oversight of risk "spatial blind spots" and their generative mechanisms hampers the development of precise proactive control strategies with existing methods.

In summary, while existing research has achieved fruitful results in mixed traffic flow characteristics, traffic conflict techniques, and safety evaluation of merging areas, several challenges remain when applying these to safety assessment of merging areas in mixed CAV traffic environments. First, there is a lack of predictive models: studies have largely focused on macroscopic performance simulations, with insufficient integration of microscopic conflict interaction mechanisms to quantitatively capture the dynamic relationship between CAV penetration rates and safety levels. Second, indicator adaptability is inadequate: the introduction of CAVs alters interaction logics, and the effectiveness of traditional conflict indicators in mixed traffic environments requires systematic validation and calibration. Third, the spatial granularity of existing methods is coarse. Conventional approaches, including hotspot analysis, typically produce static, aggregated risk maps. This fails to capture the microscopic spatial heterogeneity and dynamic evolution of risks, thereby precluding the precise, lane-level or sub-lane-level control necessary for targeted interventions.

To address these challenges, this study proposes a novel, integrated safety assessment framework that uniquely bridges conflict prediction with spatial risk distribution mapping. Unlike conventional methods that treat safety metrics in isolation, this framework systematically links predictive modeling, indicator validation, and spatial diagnostics to deliver a comprehensive, multi-resolution view of risk. Specifically, it achieves integration at three levels: (1) constructing a predictive model that quantifies the safety benefits of mixed CAV traffic as a function of penetration rates; (2) validating and calibrating conflict indicators to

ensure their relevance and sensitivity in mixed traffic environments; and (3) establishing a high-resolution spatial risk model to uncover the micro-level distribution and spatiotemporal evolution of risk hotspots—a key gap in current merging-area assessments. Ultimately, this framework advances safety evaluation from coarse, macroscopic statistics toward fine-grained, predictable, and spatially localizable risk intelligence. It thereby provides a methodologically coherent and practically usable tool for proactive safety management and system optimization in mixed CAV traffic environments.

2. Data and Methods

2.1. Study Area and Data Source

The data foundation of this study is the publicly available, high-precision Aerial Dataset for China's Congested Highways & Expressways (AD4CHE). This dataset was collected via drone aerial photography with a sampling frequency of 30 Hz. It contains multi-dimensional motion states and interaction data, including vehicle trajectories, speed, acceleration, and inter-vehicle relative positions, providing high-precision data support for microscopic traffic behavior modeling and conflict analysis [31,32].

The study area was selected as a two-lane, direct-type acceleration lane merging area on an urban expressway (as shown in Figure 1). According to the geometric information provided by the dataset, the physical acceleration lane in this area is approximately 140 m in length, with a standard lane width of 3.5 m. The mainline design speed is 60 km/h. To comprehensively capture vehicle interaction behaviors throughout the entire merging process from initiation to completion, the analysis scope (or "study section") was extended beyond the acceleration lane. It spans from the ramp nose, through the entire acceleration lane (~140 m), and continues along the corresponding mainline lanes to capture the post-merging stabilization. This defines a contiguous study section with a total length of approximately 350 m.

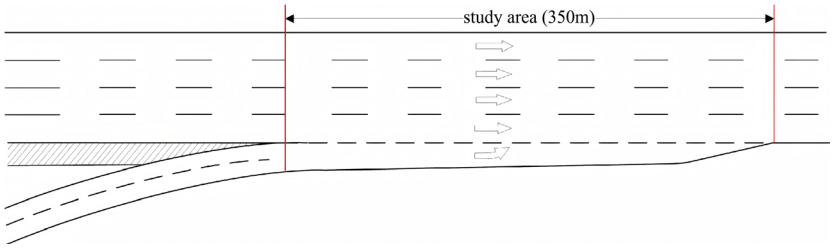


Figure 1. Schematic diagram of the two-lane direct-type acceleration lane merging area.

From the AD4CHE dataset, this study extracted data from three video clips (referred to as "merging area scenarios") numbered DJI_0001 to DJI_0003. The total recording duration of these three scenarios is approximately 900 s (totaling about 27,000 frames), covering a spatial span of 350 m. Through preprocessing steps such as coordinate correction, map-matching, and filtering on the raw trajectory data, precise sequences of position, instantaneous speed, and acceleration for all vehicles within the study scope were extracted.

Statistical analysis of the extracted trajectory data indicates that the average speed of vehicles in the study area is approximately 50 km/h (Standard Deviation: 10 km/h), and the average acceleration is approximately -0.2 m/s^2 (Standard Deviation: 0.8 m/s^2). Based on the processed high-precision trajectory data, potential traffic conflict events were further identified using indicators such as Time to Collision and Cumulative Time to Collision, establishing a reliable data foundation for subsequent modeling analysis and risk quantification.

2.2. Comprehensive Safety Risk Assessment Method for Merging Areas

Traffic Conflict Technique (TCT), which quantifies observable situations where two or more road users approach each other in space and time to such an extent that there is a risk of collision if their movements remain unchanged, effectively addresses the limitations of scarcity and lag associated with historical accident data, and has become a mainstream method for proactive traffic safety assessment [33]. In merging areas, where vehicle trajectories mandatorily converge and interactions are frequent, conflicts primarily manifest as two typical patterns: rear-end conflicts (vehicle movement direction angle $\theta < 15^\circ$) and lateral conflicts ($15^\circ \leq \theta \leq 85^\circ$). To scientifically and comprehensively quantify the safety risk in this area, it is necessary to construct a quantitative framework that integrates conflict identification, severity classification, and comprehensive assessment.

Among the various indicators in TCT, such as time headway, post-encroachment time, deceleration rate to avoid a crash, and time to collision [34–36], Time to Collision (TTC) is selected as the core identification indicator in this study due to its ability to continuously and dynamically characterize the urgency of conflict evolution. Based on the identified conflict events, the cumulative frequency curve method [25,37] is employed, using the 85th and 20th percentiles of TTC values as thresholds to classify conflicts into two severity levels: "general conflicts" and "severe conflicts", thereby distinguishing different levels of risk severity.

However, the count of conflicts of a single type or severity level is insufficient to fully reflect the overall safety condition of a merging area. To achieve a comprehensive quantification of safety levels and enable cross-scenario comparability, this study further integrates conflict type, severity, and their potential societal consequences to construct a Comprehensive Conflict Risk Index (CCRI). This index aims to aggregate multidimensional risk information, and its calculation formula is as follows:

$$\mathrm{CCRI} = 0.54 \times \left(0.14\mathrm{R_g} + 0.3\mathrm{R_s}\right) + 0.46 \times \left(0.18\mathrm{S_g} + 0.38\mathrm{S_s}\right) \quad (1)$$

where $\mathrm{R_g}$ and $\mathrm{R_s}$ represent the number of general and severe rear-end conflicts, respectively; $\mathrm{S_g}$ and $\mathrm{S_s}$ represent the number of general and severe lateral conflicts, respectively.

To clarify the derivation of the parameters for the Comprehensive Conflict Risk Index (CCRI), the following explains the rationale behind its two sets of weights, ensuring they have a clear physical meaning and statistical basis. The weights are determined by two distinct methods respectively.

(1) Conflict Severity Weights (0.14, 0.30, 0.18, 0.38): These are calculated based on the "accident conversion risk" characterized by the reciprocal of the average TTC (Time to Collision) indicator. A smaller TTC value indicates a more urgent conflict and a higher accident risk. The severity weights for the four conflict types (general/severe rear-end, general/severe lateral) within their respective categories are obtained by normalizing their risk values (calculation basis provided in Table 1).

(2) Conflict Type Weights (Rear-end: 0.54, Lateral: 0.46): These are determined based on the direct economic losses from traffic accidents. According to national traffic accident statistics from 2016–2018, the average direct economic loss per accident for rear-end collisions and lateral collisions (including sideswipe) was calculated separately. Normalization of these average losses yields the respective weights for the two conflict types, reflecting the differing severity of their potential socioeconomic consequences (calculation basis provided in Table 2).

Table 1. Severity weights for different types of traffic conflicts.

Conflict Type	General Rear-End Conflict	Severe Rear-End Conflict	General Lateral Conflict	Severe Lateral Conflict
Mean indicator value	3.17	1.41	2.32	1.10
Traffic accident probability	0.32	0.71	0.43	0.91
Weight	0.14	0.30	0.18	0.38
Mean indicator value	3.17	1.41	2.32	1.10

Note: The "Mean indicator value" (average TTC) and "Traffic accident probability" are derived from the empirical conflict dataset and historical accident records. The "Weight" values are calculated by the authors through normalizing the reciprocal of the mean TTC values, representing the relative risk of accident conversion.

Table 2. Basis for conflict type weight calculation.

Accident Category	Rear-End Accident	Lateral Accident
Direct economic loss (billion CNY)	92.46	228.68
Number ($\times 10^4$ times)	359.89	1048.49
Average economic loss ($\times 10^4$ CNY)	0.257	0.218
Weight	0.54	0.46

Note: The direct economic loss and frequency data were obtained from the [National Traffic Accident Statistics Annual Report] (2016–2018) [38,39]. The "Average economic loss" and "Weight" were calculated by the authors based on the raw statistics to reflect the socioeconomic impact of different collision types.

It should be noted that the assignment of weights in the CCRI is based on a two-fold rationale aiming to balance the physical characteristics of conflicts with their potential socioeconomic impacts. The severity weights (0.14, 0.30, 0.18, 0.38) are derived from the physical metric of TTC (Time to Collision). A smaller TTC value indicates a higher probability of immediate collision, thereby justifying the higher weights assigned to severe conflicts compared to general ones within the same category.

Regarding the conflict type weights (Rear-end: 0.54, Lateral: 0.46), these are calibrated based on the average direct economic losses associated with actual traffic accidents (as shown in Table 2). While it is acknowledged that not all conflicts result in accidents, using accident losses serves as a pragmatic surrogate to reflect the relative severity of different conflict types in terms of potential property damage and human injury. This approach assumes that conflict types responsible for higher average economic losses in the event of an accident inherently possess greater destructive potential and societal consequence. To ensure the validity of this approach, the weights have been normalized to ensure they sum to unity within their respective categories (severity or type), thereby mitigating scale bias.

Through the above weighting approach, this comprehensive index integrates the frequency of conflicts, the severity of real-time risk, and their potential socioeconomic impact. It achieves a transition from single-indicator measurement to a multi-dimensional, structured comprehensive assessment of safety risk in merging areas, providing a core quantitative basis for subsequent in-depth safety analysis.

2.3. Traffic Simulation Validation Method

To systematically obtain traffic conflict data across a range of CAV penetration rates, a realistic simulation of a two-lane freeway merging area was developed using SUMO. This environment provided the data foundation necessary for subsequent conflict modeling and safety assessment. In the context where real-world mixed CAV traffic data is difficult to acquire, microscopic simulation provides a reliable means for generating controllable and reproducible experimental data.

2.3.1. Simulation Environment Setup and Parameter Calibration

(1) Basic Traffic Flow Settings. Based on the actual geometric parameters from the AD4CHE dataset, a road network model consistent with the measured scenario was constructed using SUMO's Netedit tool. To simulate the dynamic traffic demand of the merging area, a total of 6 traffic flows were defined on the mainline and the ramp. The simulation duration was set to 4000 s to sufficiently eliminate random fluctuations. The vehicle composition, flow rate, routing information, and other details for each traffic flow were calibrated based on measured data (see Table 3). The "Generation probability" for each flow, a core stochastic input parameter, was calculated by converting the observed hourly traffic volume from the AD4CHE dataset into a per-second probability of vehicle generation. This ensures that the simulated traffic demand quantitatively replicates the real-world conditions. Key parameters, including the passenger car-to-truck ratio and the ramp flow ratio, collectively constitute the baseline traffic scenario for subsequent penetration rate control experiments.

Table 3. Basic simulation traffic flow settings.

Flow ID	Vehicle Type	Origin Link	Route	Generation Probability	Description
flow1	Passenger car	Mainline (E0)	E0 → E1 → E2	0.80	Mainline through passenger car flow
flow2	Passenger car	Mainline (E0)	E0 → E1 → E2	0.70	Mainline through passenger car flow
flow3	Passenger car	Mainline (E0)	E0 → E1 → E2	0.75	Mainline through passenger car flow
flow4	Passenger car	Ramp (E3)	E3 → E1 → E2	0.85	Ramp merging passenger car flow
flow5	Truck	Mainline (E0)	E0 → E1 → E2	0.06	Mainline through truck flow
flow6	Truck	Ramp (E3)	E3 → E1 → E2	0.01	Ramp merging truck flow

Note on Generation Probability: The values in the "Generation probability" column are derived from the AD4CHE dataset. They are calculated as the number of vehicles per hour for a specific flow divided by 3600 s, representing the probability of a vehicle being generated in each simulation second. The sum of probabilities from all flows determines the total simulated traffic volume. This parameterization was validated to ensure the aggregate simulated flow rates matched the measured macroscopic traffic conditions.

(2) Vehicle Types and Car-Following Behavior Parameters. To accurately simulate mixed traffic flow, the parameters for the car-following and lane-changing models of both human-driven vehicles and CAVs were calibrated separately. For human-driven vehicles, the Intelligent Driver Model (IDM) was used as the car-following model, and the LC2013 model was used as the lane-changing model. Through iterative optimization, the optimal values for key parameters such as acceleration, deceleration, and minimum safe spacing were determined (see Table 4).

For Connected and Automated Vehicles (CAVs), a Cooperative Adaptive Cruise Control (CACC) model and a lane-changing model with a cooperative decision-making mechanism were employed to reflect their vehicle-to-vehicle communication and coordinated control characteristics. The CACC model parameters for CAVs in this study were determined based on the CoEXist project and related research [40]. Using Helmond, the Netherlands, as the test site, this project collected real-world operational data from automated vehicles, focusing on analyzing their car-following behavioral characteristics and optimizing simulation model parameters based on empirical analysis results. The specific parameter settings are shown in Table 5 [41,42].

Table 4. Parameter calibration results for the IDM and LC2013 models.

Model	Parameter	Description	Calibrated Value
IDM car-following model	Veloc	Desired speed (m/s)	33.3
	Accel	Maximum acceleration (m/s^2)	1.2
	Decel	Comfortable deceleration (m/s^2)	2.8
	minGap	Minimum safe gap (m)	2
	tau	Desired time headway (s)	1.3
LC2013 lane-changing model	lcAssertive	Lane-change assertiveness	1.5

Table 5. Parameter settings for automated vehicle simulation models.

Model	Parameter	Description	Value
CACC Model	minGap	Minimum gap (m)	0.5
	Accel	Acceleration (m/s^2)	2.0
	Decel	Deceleration (m/s^2)	4.0
	emergencyDecel	Emergency deceleration (m/s^2)	9.0
	sigma	Driver proficiency	0.0
	tau	Time headway (s)	0.7
LC2013	lcCooperative	Cooperative lane-changing	1
	lcSpeedGain	Speed gain consideration	1
	lcAssertive	Acceptance of reduced gaps	1

The parameter calibration strategy in this study serves two distinct but complementary purposes to ensure the validity of the mixed traffic simulation. First, calibrating the Human-Driven Vehicle (HDV) models (IDM and LC2013) against the real-world AD4CHE dataset aims to faithfully reproduce the baseline traffic flow characteristics and driver heterogeneity. Second, and critically, to avoid the pitfall of extrapolating HDV parameters to high penetration rates of Connected and Automated Vehicles (CAVs), the CAV behaviors are instead governed by parameters derived from the empirical CoExist project [35]. This ensures that simulated CAV interactions (e.g., smaller time gaps in cooperative driving) are based on real-world automated vehicle operations, not theoretical assumptions. Therefore, while microscopic simulation faces inherent challenges in predicting absolute safety outcomes, this parameter setup provides a reasonable and methodologically sound approximation for evaluating the relative changes in safety and efficiency across different CAV penetration rates.

2.3.2. Model Validation Method and Results

To evaluate the reliability of the simulation model, the average travel time, the number of rear-end conflicts, and the number of lateral conflicts were selected as the core validation metrics. Given the inherent randomness of microscopic traffic conflict events, establishing a reasonable and acceptable error margin for model validation is crucial. Synthesizing related practices, this study defines a relative error (E) not exceeding 15% as the acceptable validation criterion. The relative error is calculated as follows:

$$E = \frac{|x_1 - x_2|}{x_1} \times 100\% \quad (2)$$

where x_1 represents the actual (observed) value, and x_2 represents the simulated value.

The validation results (see Table 6) indicate that the relative errors for all metrics are controlled within 15%, meeting the preset standard. Specifically: (1) The error for average travel time ranges between 5.3% and 9.4%, showing stable consistency across different lanes. This demonstrates the model's high reliability in replicating macroscopic operational

efficiency. (2) The errors for the number of rear-end and lateral conflicts are 12.6% and 14.1%, respectively. While these are the largest among all metrics, they remain within the acceptable range, indicating the model's effectiveness in capturing the key characteristics of microscopic interactions and safety risks. In summary, the constructed simulation model can reliably replicate the traffic operation and conflict characteristics of the real-world merging area, providing a solid data foundation for subsequent research.

Table 6. Simulation model validation results.

Validation Metric	Lane ID	Actual Value	Simulated Value	Relative Error (%)
Average travel time (s)	1	10.45	9.468	9.4
	2	13.35	12.16	8.9
	3	14.63	13.51	7.7
	4	10.63	9.91	6.8
	5	9.27	8.79	5.3
Number of rear-end conflicts	1–5	243	212	12.6
Number of lateral conflicts	1–5	202	230	14.1

3. Traffic Conflict Prediction Model for Merging Areas

To construct a traffic conflict prediction model for merging areas under mixed traffic flow conditions, this study first utilizes a validated microscopic simulation model and employs orthogonal experimental design to systematically obtain multi-scenario conflict data. It then analyzes the influence mechanisms of key factors, and based on this analysis, establishes a negative binomial regression prediction model. This model serves as the core foundation for achieving quantitative safety assessment and prediction in merging areas.

3.1. Simulation and Data Acquisition Based on Orthogonal Experimental Design

To systematically obtain traffic conflict data under mixed traffic conditions and to efficiently analyze the influence of multiple factors, this study employs an orthogonal experimental design. A full factorial design for five factors at five levels would require 3125 (5^5) simulation runs, which is computationally prohibitive for the high-fidelity microscopic simulation used. The orthogonal design significantly reduces the number of required runs while ensuring a balanced and representative exploration of the factor space, allowing for the reliable estimation of main effects. The L25 orthogonal array was selected, generating 25 distinct scenario combinations (see Table 7). This approach provides a robust foundation for the subsequent development of a statistical prediction model focused on the primary influences of each factor. It is acknowledged that this design is most efficient for estimating main effects; the exploration of higher-order interaction effects, while possible to a limited extent, was not the primary focus of this screening stage.

(1) Influencing Factors and Level Design: Five key influencing factors were selected: traffic volume (Q), CAV penetration rate (AR), merging ratio (CR), acceleration lane length (L), and truck proportion (TP). The rationale for this selection lies in their established impact on merging-area safety: Q governs traffic density and interaction frequency; AR defines the mixed-traffic interaction logic; CR influences competitive maneuvering intensity; L determines the physical space for merging; and TP introduces vehicle heterogeneity affecting traffic stability.

To systematically examine their effects within a computationally feasible framework, an L_{25} orthogonal array was employed. Accordingly, each factor was assigned five levels (see Table 7). This configuration ensures a balanced and efficient exploration of the factor space. The specific level values were strategically determined based on the measured ranges from the AD4CHE dataset and relevant highway design specifications, ensuring

the scenarios are both representative of real-world conditions and capable of covering a spectrum of traffic states from free flow to congestion. This design provides the necessary granularity to model the nuanced influence of each factor on safety outcomes.

(2) Experimental Scheme and Simulation Execution: An L25 (5^6) orthogonal array was selected to design the experiments. This standard array is specifically suited for screening experiments involving multiple factors (up to six) at five levels each. For the present study with five key factors, it provides a balanced and orthogonal design with only 25 required runs. This is the minimal configuration that allows each level of every factor to be tested an equal number of times and combined uniformly with the levels of all other factors, thereby ensuring an efficient and statistically reliable estimation of the main effects for each factor. This study utilized five columns of this array to scientifically determine 25 sets of balanced and representative simulation scenario combinations. All scenarios ran sequentially on the SUMO platform, with each simulation lasting 4000 s, including a 400 s warm-up period to eliminate the influence of initial states. During the simulations, the TraCI interface facilitated the real-time collection and recording of the number of both general and severe rear-end and sideswipe conflicts in each scenario, thereby providing a systematic and efficient data foundation for constructing the subsequent conflict prediction model.

Table 7. Orthogonal experimental factors and level design.

Influencing Factors	Notation	Factor Level				
		1	**2**	**3**	**4**	**5**
Traffic volume (veh/h)	Q	4500	5000	5500	6000	6500
CAV penetration Rate (%)	AR	10	20	30	40	50
Merging ratio (%)	CR	15	20	25	30	35
Lane length (m)	L	160	190	220	250	280
Truck proportion (%)	TP	1	2	3	4	5

3.2. Analysis of Key Influencing Factors of Traffic Conflicts

Drawing on simulation data from orthogonal experiments, this study analyzes the effects of five key factors on the frequency of four traffic conflict types in the merging area. These factors are: traffic volume (Q), CAV penetration rate (AR), merging ratio (CR), acceleration lane length (L), and truck proportion (TP). The results are shown in Figures 2–6.

(1) Influence of Traffic Volume

As shown in Figure 2, as traffic volume increases from 4500 veh/h to 6500 veh/h, all types of conflicts exhibit a monotonically increasing trend. Among them, the severe sideswipe conflict shows the highest growth rate, indicating that it is the most sensitive to changes in traffic volume. Within the 4500–5000 veh/h range, the traffic flow transitions from free flow to stable flow, and the number of conflicts begins to increase significantly. When the traffic volume exceeds 5500 veh/h and enters a congested flow state, the reduced speed differential between vehicles leads to a decrease in interaction intensity, causing the growth rate of conflict frequency to gradually level off. This pattern verifies that the safety risk in the merging area increases nonlinearly as capacity is approached, and the rate of risk exacerbation slows down under saturated flow conditions.

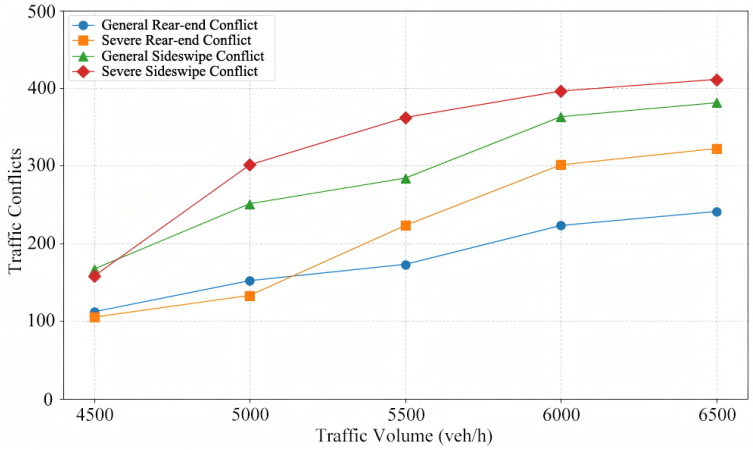


Figure 2. Traffic volume—traffic conflicts.

(2) Influence of CAV Penetration Rate

As shown in Figure 3, the introduction of CAVs leads to a significant improvement in safety. As the penetration rate increases from 10% to 50%, all types of conflicts show a continuous reduction, with the severe sideswipe conflict exhibiting the most pronounced decline rate. When the penetration rate reaches approximately 30%, a clear inflection point appears on the conflict curve. At a penetration rate of 50%, the number of each type of conflict is reduced by approximately 50% to 75% compared to the 10% baseline scenario. This indicates that the cooperative control capability of CAVs plays a decisive role in enhancing the safety level of the merging area.

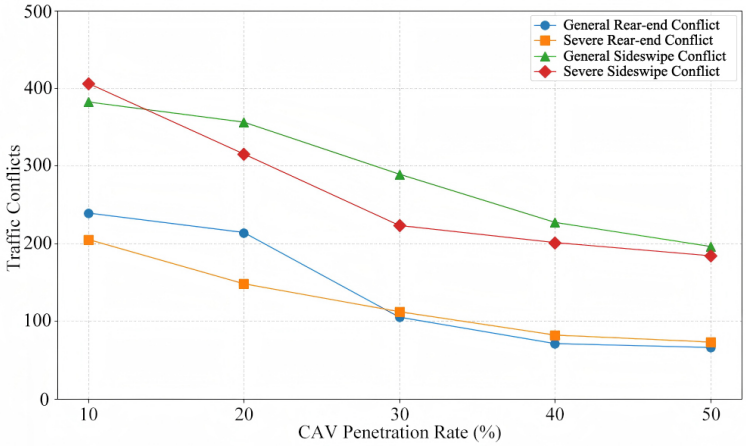


Figure 3. CAV penetration rate—traffic conflicts.

(3) Influence of Merging Ratio

As shown in Figure 4, an increase in the merging ratio from 0.15 to 0.35 will lead to a rise in all conflict types. Among them, severe sideswipe conflict exhibits the most dramatic response, characterized by the steepest growth slope. This is directly attributed to the fact that a higher merging ratio results in more vehicles entering from the ramp, which significantly intensifies lateral interactions and competitive maneuvers between vehicles, thereby leading to a sharp increase in sideswipe conflict risk.

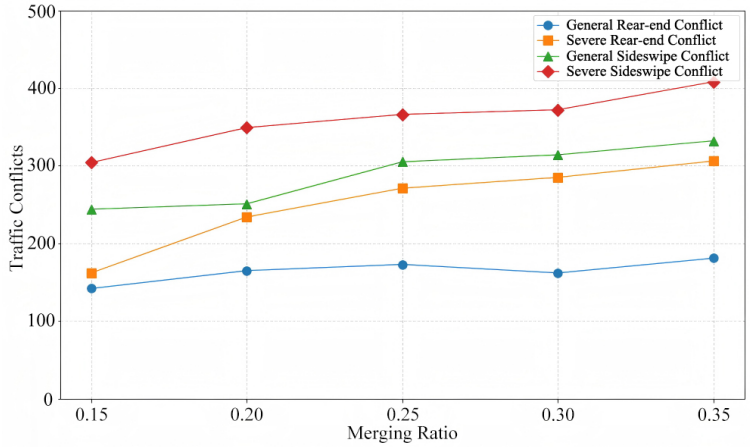


Figure 4. Merging ratio—traffic conflicts.

(4) Influence of Lane Length

As shown in Figure 5, increasing the length of the acceleration lane effectively enhances safety in the merging area. As the lane length increases from 160 m to 280 m, all types of traffic conflicts decrease significantly. Among them, the reduction in sideswipe conflicts, particularly severe ones, is the most pronounced. This benefit is attributed to the longer acceleration lane providing sufficient space for vehicles to execute smoother merging maneuvers, thereby effectively mitigating the intensity of lateral interactions. Concurrently, rear-end conflicts are also reduced owing to the increased space for speed adjustment and the resultant more stable car-following behavior.

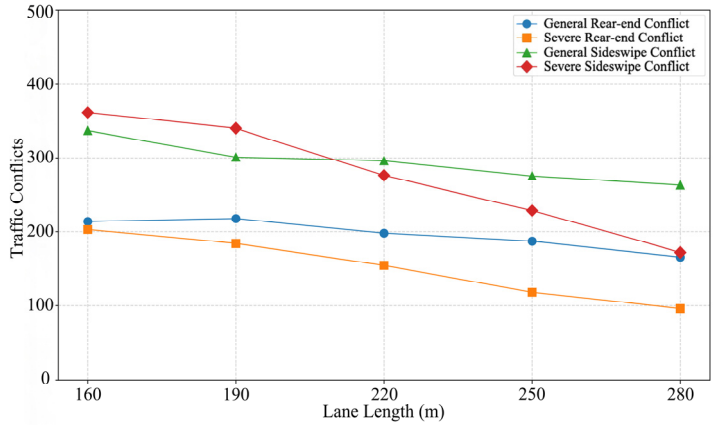


Figure 5. Lane length—traffic conflicts.

(5) Influence of Truck Proportion

Within the relatively low variation range set in this study (1% to 5%), Figure 6 shows that the frequencies of the four types of traffic conflicts do not exhibit a statistically significant monotonic pattern as the truck proportion increases, with their fluctuation range being relatively limited. This finding indicates that, in this low-proportion scenario, the truck proportion is not a key dominant factor influencing conflicts in the merging area. Its disruptive effect may be diluted by the driving behavior of the predominant passenger car population.

The comprehensive analysis reveals that traffic volume, CAV penetration rate, merging ratio, and acceleration lane length are the key factors influencing conflicts in the merging area, providing a direct basis for the selection of independent variables in the subsequent prediction model.

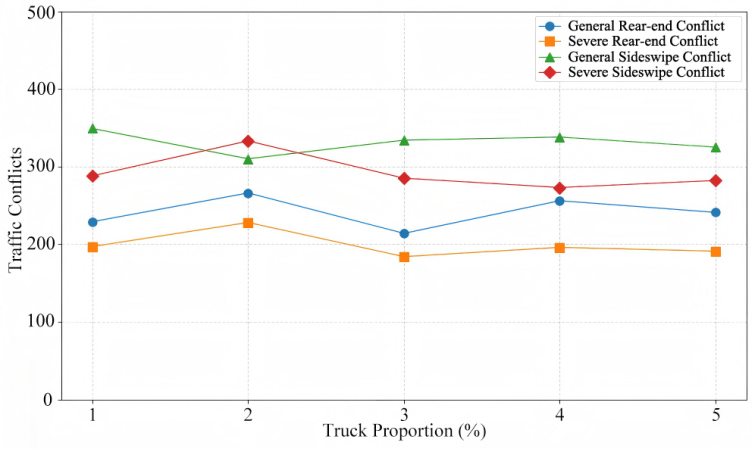


Figure 6. Truck proportion—traffic conflicts.

3.3. Development of a Traffic Conflict Prediction Model Based on Negative Binomial Regression

Based on the multi-scenario traffic conflict data acquired from orthogonal experiments, this section develops a negative binomial regression model. The model aims to achieve accurate predictions of the occurrence counts of four conflict types (general/severe rear-end, general/severe sideswipe) in the merging area, thereby providing a core modeling tool for subsequent quantitative safety assessment. It is important to clarify that the purpose of developing this statistical prediction model is not to replace the aforementioned simulation model. While microscopic traffic simulation can capture the details of vehicle interactions, it is also computationally expensive. Moreover, the relationship between its outputs (e.g., conflict counts) and input parameters (e.g., Q, AR) is implicit, making direct analysis and rapid scenario testing challenging. By fitting a negative binomial regression model to the simulation data, we aim to establish a lightweight, interpretable, and computationally efficient surrogate model. This approach offers two core advantages: (1) It directly quantifies the marginal effect of each influencing factor on conflict frequency, clarifying the direction and magnitude of its impact, thereby providing a clear mathematical basis for mechanistic analysis; (2) it enables instantaneous prediction of conflict counts for any traffic scenario within the calibrated parameter range, significantly enhancing the efficiency of large-scale scenario screening and safety assessment, and providing the essential input for the subsequent development of the composite risk index and spatial distribution model.

3.3.1. Basis for Model Selection

Traffic conflict data, being count variables, are typically modeled using Poisson series regression models. In this study, the variance of the data for all four conflict types is significantly greater than their mean, indicating pronounced over-dispersion, which violates the equidispersion assumption underlying Poisson regression. Consequently, the negative binomial regression model is selected as the modeling foundation, as it can flexibly handle over-dispersion by introducing a dispersion parameter (α).

3.3.2. Variable Screening and Model Construction

The initial modeling effort focuses on quantifying the individual (main) effects of the key influencing factors to establish a foundational and interpretable predictive relationship. While interaction and quadratic effects can provide deeper mechanistic insights, their reliable estimation would require a more extensive experimental design specifically tailored for that purpose. The L_{25} orthogonal array employed in this study is optimized for the efficient estimation of main effects, which aligns with the primary objective of this screening

and modeling stage. The investigation of potential higher-order effects is suggested as a valuable direction for future research.

First, a multicollinearity diagnosis was performed for the five key influencing factors: traffic volume (Q), CAV penetration rate (AR), merging ratio (CR), lane length (L), and truck proportion (TP). As shown in Table 8, the variance inflation factor (VIF) values for all variables are significantly lower than 5 (the maximum is 1.087), indicating negligible multicollinearity among the independent variables. Therefore, all of them can be included as candidate variables in the preliminary model. Subsequently, using the aforementioned factors as independent variables and the respective counts of the four conflict types as dependent variables, a stepwise regression method (with the significance levels for entry and removal set at 0.05 and 0.10, respectively) was employed for variable screening and negative binomial regression model construction.

Table 8. Multicollinearity diagnostics.

Influencing Factors	Unstandardized Coefficient		Beta	t	Significance	Collinearity Statistics	
	B	Standard Error				Tolerance	VIF
(Constant)	−110.292	37.468	-	−2.944	0.008	-	-
Traffic volume	0.03	0.005	0.691	7.464	0.000	1.000	1.000
CAV penetration rate	−119.000	24.517	−0.450	−4.854	0.000	1.000	1.000
Merging ratio	139.130	50.089	0.263	2.778	0.012	0.958	1.043
Lane length	−0.333	0.125	−0.252	−2.658	0.016	0.958	1.043
Truck proportion	−221.739	255.612	−0.084	−0.867	0.397	0.920	1.087

Based on the significant coefficients presented in Table 8, the final prediction models established for the four types of conflicts are as follows:

(1) General Rear-end Conflict: $N_1 = \exp(1.95 + 0.00054Q - 1.64AR + 1.04CR - 0.30L)$
(2) Severe Rear-end Conflict: $N_2 = \exp(1.69 + 0.00056Q - 1.60AR + 1.16CR - 1.08L)$
(3) General Sideswipe Conflict: $N_3 = \exp(2.64 + 0.00048Q - 1.52AR + 1.17CR - 0.53L)$
(4) Severe Sideswipe Conflict: $N_4 = \exp(2.26 + 0.00051Q - 1.46AR + 1.37CR - 1.20L)$

3.3.3. Model Validation and Result Analysis

To evaluate the prediction accuracy and generalization ability of the models, a hold-out method was employed for validation. From the 25 sets of orthogonal experimental data, 5 sets (20% of the total data) were randomly selected to form an independent test set, while the remaining 20 sets (80%) were used for model training. The validation results show that the relative error for all four types of conflict prediction models is controlled within 15% (with a maximum error of 12.3%), indicating that the models possess good prediction accuracy and robust generalization ability.

The parameter estimation results for the final models are shown in Table 9, which quantifies the specific influence mechanisms of each factor on conflict risk: (1) Traffic volume has a highly significant positive effect on all conflict types, which is consistent with the common understanding that increased traffic density leads to more interaction opportunities. (2) CAV penetration rate shows a highly significant negative effect in all models, with a relatively large absolute coefficient. This clearly confirms that the introduction of CAVs can substantially reduce conflict risk, constituting a key factor for enhancing safety in merging areas. (3) An increase in the merging ratio significantly raises the number of conflicts, reflecting that greater merging demand intensifies disturbance to the mainline traffic flow. Increasing the length of the acceleration lane has a significantly positive impact on safety, providing a basis for optimizing the geometric design of merge areas.

Table 9. Goodness-of-fit results for the traffic conflict prediction models.

Influencing Factors	General Rear-End Conflict	Severe Rear-End Conflict	General Sideswipe Conflict	Severe Sideswipe Conflict
Traffic volume(Q)	0.00054 ***	0.00056 ***	0.00048 ***	0.00051 ***
CAV penetration rate(AR)	−1.64 ***	−1.60 ***	−1.52 ***	−1.46 ***
Merging ratio(CR)	1.04 **	1.16 *	1.17 *	1.37 *
Lane length(L)	−0.30 ***	−1.08 **	−0.53 ***	−1.20 ***
Constant	1.95 ***	1.69 **	2.64 ***	2.26 ***

Note: * $p < 0.05$, ** $p < 0.01$, *** $p < 0.001$.

These quantitative conclusions derived from the econometric models and the trend analysis results from Section 3.2 mutually corroborate, providing not only statistical empirical support but, more importantly, offering specific directions and magnitudes of the effects of each influencing factor, thereby achieving a leap from qualitative understanding to quantitative description of the conflict generation mechanism.

4. Safety Assessment Integrating Conflict Prediction and Risk Spatial Distribution

4.1. Development of an Internal Risk Distribution Model for Merging Areas

A granular safety assessment of merging areas requires spatially allocating macro-level conflict predictions to the micro-scale physical layout of the interchange. To this end, building upon the comprehensive conflict risk index developed earlier, this study employs a spatial discretization method to establish an internal risk distribution model for merging areas. The aim is to associate quantitative safety risk with specific spatial locations, thereby revealing the micro-level distribution and aggregation characteristics of risk. This model bridges macro-level conflict prediction and micro-scale spatial diagnosis, enabling the first-ever visualization of risk hotspots in merging areas.

4.1.1. Methodology for Constructing the Risk Distribution Model

To achieve the aforementioned objective, the study area of the merging zone is first discretized into a series of regular rectangular grid cells (m × n). This is done at 10 m intervals along the direction of travel and with single-lane intervals across the lane cross-section. The risk level of each grid cell is quantified by the CCRI calculated from all traffic conflicts occurring within that region. Consequently, the safety state of the merging area is transformed into a spatial risk matrix (Equation (3)), thereby mapping macro-level conflict frequencies onto a micro-level spatial distribution.

$$R^{*} = \begin{bmatrix} r_{11} & r_{12} & \cdots & r_{1n} \\ r_{21} & r_{22} & \cdots & r_{2n} \\ \vdots & \vdots & \vdots & \vdots \\ r_{m1} & r_{m2} & \cdots & r_{mn} \end{bmatrix} \quad (3)$$

where R* is the risk distribution matrix for the merging area; r_{mn} is the CCRI of the grid cell located at the *m*-th row (longitudinal segment) and the *n*-th column (lane).

4.1.2. Visual Validation and Spatial Evolution Analysis of Risk Distribution

To validate the constructed model and decipher the evolution of risk patterns, the spatial risk matrices (from Equation (3)) for scenarios with CAV penetration rates from 10% to 50% were converted into risk heatmaps (Figures 7–11). This visualization intuitively

confirms the model's capability to resolve micro-scale spatial heterogeneity and, more critically, reveals a complete dynamic evolution of risk patterns as CAV penetration increases. The observed evolution follows two distinct phases:

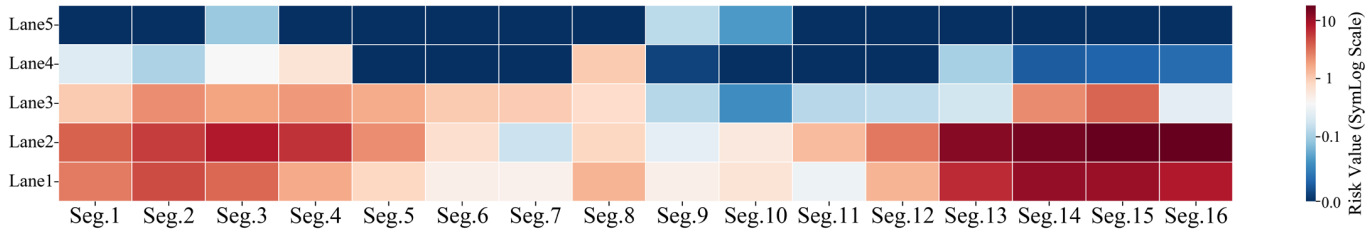


Figure 7. Distribution of the comprehensive conflict risk under 10% CAV penetration rate.

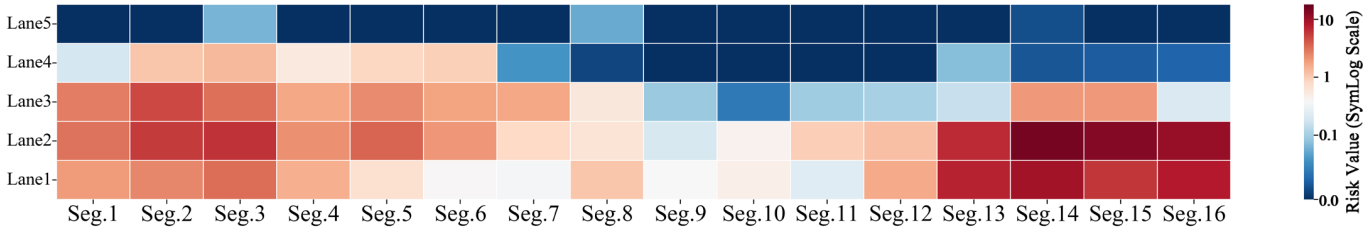


Figure 8. Distribution of the comprehensive conflict risk under 20% CAV penetration rate.

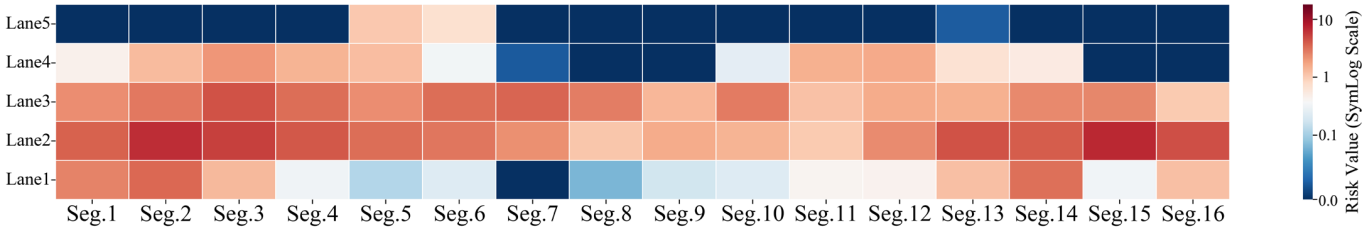


Figure 9. Distribution of the comprehensive conflict risk under 30% CAV penetration rate.

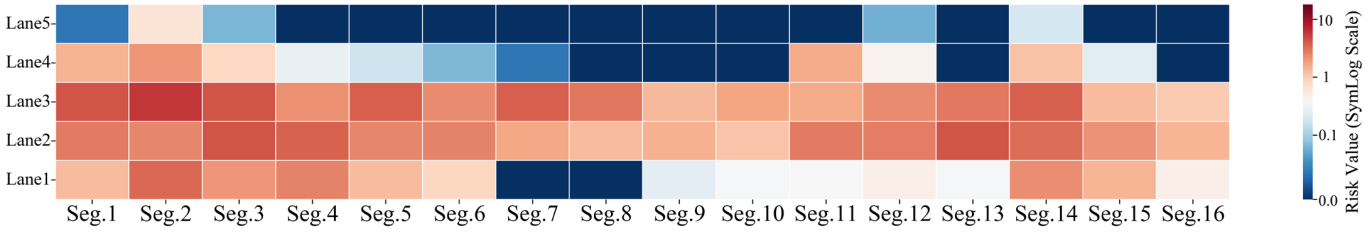


Figure 10. Distribution of the comprehensive conflict risk under 40% CAV penetration rate.

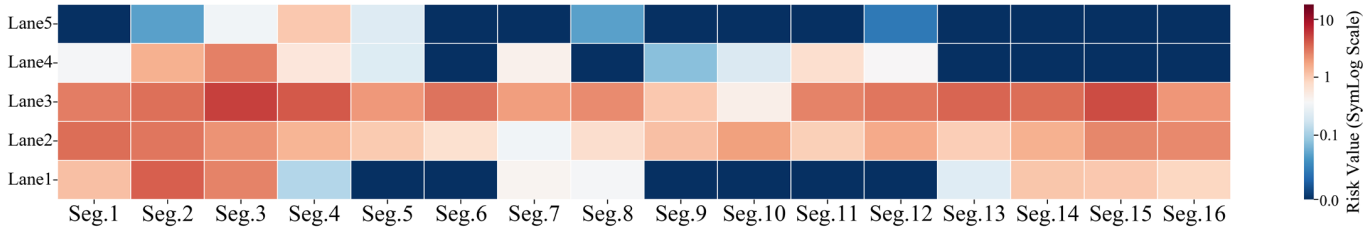


Figure 11. Distribution of the comprehensive conflict risk under 50% CAV penetration rate.

(1) Low CAV penetration phase (10–20%): Risk Concentration at Geometric Bottlenecks. As shown in Figures 7 and 8, high-risk areas (red) concentrate sharply in the merging zone—specifically at the acceleration lane terminus and the adjacent mainline Lane 2. This pattern stems from competition among human-driven vehicles for limited merging gaps under spatiotemporal constraints, triggering frequent emergency car-following and forced

lane-changing maneuvers. Consequently, this zone acts as a static geometric bottleneck, representing a persistent safety black spot.

(2) Medium-to-high CAV penetration phase (30–50%): Risk Shift to Behavioral Interaction Interfaces. When CAV penetration reaches 30% and above (Figures 9–11), the risk pattern undergoes a fundamental reconfiguration. While high-risk zones shrink substantially (indicating overall safety improvement), risk hotspots migrate systematically from the merging zone to the mid-section of mainline Lane 3. This shift occurs because CAVs, utilizing V2V communication for coordinated lane-changing and speed harmonization, complete merging maneuvers earlier and more smoothly, thereby alleviating the original bottleneck. Simultaneously, Lane 3 becomes a core zone where CAV platoons and non-merging human-driven vehicles engage in sustained parallel travel and complex interactions, forming a new dynamic behavioral risk interface.

This spatial evolution does more than validate the model; it reveals the underlying mechanism of CAV-driven safety improvement. Safety is enhanced not through a uniform reduction of risk, but via a restructuring of traffic operations that transfers and mitigates risk. The identified paradigm of shifting from static geometric bottlenecks to dynamic behavioral interfaces explains how CAVs change the safety landscape, providing a theoretical basis for optimizing CAV-aware traffic management. Furthermore, it directly informs the selection of key spatial metrics (e.g., conflict dispersion in Lane 3) for the subsequent safety assessment framework, marking a leap from macro-level statistics to micro-scale spatial insight.

4.2. Safety Evaluation Model and Classification Based on Spatial Risk Distribution

To overcome the limitations of traditional single-metric evaluations based solely on conflict frequency, and to achieve a comprehensive assessment ranging from "macro-level intensity" to "micro-level distribution", this study integrates conflict frequency, severity, and spatial distribution characteristics to construct a two-tier comprehensive safety evaluation index system and employs a grey variable-weight clustering method to perform the grade evaluation.

4.2.1. Development of the Evaluation Index System

Based on the previous analysis of the spatial risk distribution in merging areas, the following four core indicators are selected to construct the evaluation system:

Total Number of Conflicts (K1): The aggregate count of traffic conflicts occurring within the merging area during the statistical period. It directly reflects the frequency of accident risk in the area.

Conflict Density (K2): The number of conflicts per unit area (conflicts/m^2). This metric eliminates the influence of variations in the geometric dimensions of the merging area and characterizes the relative concentration of risk.

Comprehensive Conflict Risk Index (K3): This adopts the CCRI index developed earlier, which integrates weighting factors for conflict type and severity to provide a composite quantification of risk level.

Standard Deviation of Conflict Positions on Lane 3 (K4): This metric calculates the standard deviation of conflict point locations within the key risk area (Lane 3). Derived from the pattern of "risk hotspot migration to Lane 3" identified in the previous analysis, it is used to characterize the spatial dispersion of conflicts, reflecting the orderliness of traffic flow.

4.2.2. Grey Variable-Weight Clustering Evaluation Method

To address the uncertainty of information and the nonlinear relationships among indicators in safety evaluation, the grey variable-weight clustering method is selected. This method employs whitening weight functions to handle the fuzziness in the indicators.

Moreover, it can dynamically adjust the clustering weight assigned to each indicator based on the safety level (grey class) to which the sample data belongs. Consequently, the method is able to more sensitively reflect how the importance of each indicator varies under different safety states. The specific procedural steps are as follows.

(1) Data standardization: Standardize the evaluation indicators to eliminate the influence of dimensionality.

(2) Determination of whitening weight functions: The method classifies the safety status into four grades (A to D) and determines the corresponding thresholds and whitening weight functions for each grade based on the data distribution.

(3) Calculation of variable-weight clustering coefficients: The grey variable-weight clustering coefficient is determined by the whitening weight function value of each index and its dynamic weight, and its calculation formula is as follows [38]:

$$\sigma_{ik} = \sum_{j=1}^{m} f_{jk}(x_{ij})\eta_{jk} \quad (4)$$

where σ_{ik} is the clustering coefficient for object i belonging to grey class k, $f_{jk}(x_{ij})$ is the whitening weight function value, η_{jk} is the clustering weigh.

(4) Determination of Safety Grade: According to the principle of maximum membership degree, the safety grade for each sample is determined by assigning it to the grade with the maximum clustering coefficient.

4.2.3. Determination of Safety Grade Clustering Results and Thresholds

Applying the previously constructed comprehensive safety evaluation index system and the grey variable-weight clustering method, this section classifies the safety level of the merging area. The aims are to determine critical thresholds and to reveal the traffic flow characteristics underlying each safety grade.

(1) Safety grade clustering results

Grey variable-weight clustering classified the 25 scenarios into four safety grades: 9 as Excellent (Grade A), 8 as Good (B), 5 as Fair (C), and 3 as Poor (D). The clustering weights (Table 10) uncover grade-specific indicator importance: for example, the Standard deviation of conflict positions on Lane 3dominates Grade A (weight = 0.293), reflecting its critical role in identifying "orderly, low-risk" traffic flow with sparse, homogeneous conflicts; in contrast, Conflict density strongly signals Grade D (weight = 0.261), indicating its sensitivity to "disordered, high-risk" conditions with dense, unstable conflicts. This objective, data-driven classification aligns with independent expert assessments (e.g., traffic engineers' qualitative evaluations of safety levels), validating the model's ability to differentiate safety grades.

Table 10. Clustering weights of each evaluation indicator under different safety grades.

Evaluation Indicators	Safety Grade A	Safety Grade B	Safety Grade C	Safety Grade D
Total number of conflicts	0.224	0.251	0.240	0.235
Conflict density	0.257	0.265	0.241	0.261
Comprehensive conflict risk index	0.225	0.247	0.243	0.234
Standard deviation of conflict positions on lane 3	0.293	0.236	0.275	0.270

(2) Safety grade thresholds and grade-specific characteristics

Based on the upper distribution limits of evaluation indicator values across safety grades (from the clustering results), key thresholds for classifying merging area safety are determined (Table 11). These thresholds serve as a rapid diagnostic tool for practitioners: for instance, a scenario with >1460 total conflicts and >0.384 conflict density is classified as Grade D (Poor), triggering immediate interventions (e.g., ramp metering, speed guidance) to mitigate risks.

Table 11. Safety grade classification thresholds for merging areas.

Safety Grade	Total Number of Conflicts	Conflict Density	Comprehensive Conflict Risk Index	Standard Deviation of Conflict Positions on Lane 3
A (Excellent)	≤472	≤0.168	≤74.245	≤25.475
B (Good)	≤877	≤0.319	≤108.560	≤32.464
C (Fair)	≤1460	≤0.384	≤176.661	≤53.687
D (Poor)	>1460	>0.384	>176.661	>53.687

Typical traffic flow characteristics and management implications of each safety grade:

Grade A (Excellent): Traffic flow is stable and smooth, characterized by sparse, homogeneous conflicts (e.g., routine car-following). This state occurs under ideal conditions, including high CAV penetration (which leverages cooperative driving), low traffic volume, or sufficient lane length. The recommended management focus is to maintain the current control strategy, implying that no active intervention is typically needed.

Grade B (Good): Traffic flow experiences minor disturbances (e.g., occasional lane changes) but remains fundamentally stable. This condition is typical of scenarios with moderate CAV penetration (enabling partial coordination) and balanced traffic demand. The management focus should be on monitoring traffic dynamics and implementing proactive guidance measures, such as variable message signs, if congestion appears imminent.

Grade C (Fair) & Grade D (Poor): Traffic flow is disordered, with frequent, high-risk conflicts (e.g., forced lane changes, rear-end collisions). This arises under adverse conditions, primarily low CAV penetration (resulting in human-driven dominance), high traffic volume, or the presence of geometric bottlenecks. The management focus must involve deploying active interventions (e.g., ramp metering to reduce inflow and speed guidance to harmonize CAV-human speeds) and prioritizing increased CAV penetration to restore order.

The established safety grade system represents a paradigm shift in merging area safety assessment, from macro-level statistical summaries to micro-level spatial–temporal insights (via spatial distribution indicators of conflict risk). By integrating spatial distribution indicators and dynamic weighting, this system enables: (1) precise localization of risk hotspots (e.g., Lane 3 as a dynamic interaction interface), (2) quantitative grade diagnosis (e.g., using conflict density to flag Grade D), and (3) targeted management strategies (e.g., CAV penetration optimization for Grade D). This transcends traditional macro-level evaluations, providing a practical, theory-driven tool for mixed-traffic merging area management.

5. Model Validation and Comprehensive Discussion

5.1. Case Validation and Result Analysis

This section illustrates the integrated application of the proposed models through a case study, detailing the process of evaluating CAV penetration impacts to demonstrate their practical utility.

The baseline conditions are selected as: traffic volume 5500 veh/h, merging ratio 25%, acceleration lane length 220 m, and truck proportion 3%. Six scenarios are configured by increasing the CAV penetration rate from 0% (baseline) to 50%. The application process entails three stages: conflict prediction, followed by risk calculation, culminating in safety evaluation. The application results (Table 12) indicate the following. (1) Validity: The baseline scenario (0% CAV) is rated as Grade D, which aligns with the actual congested conditions of the case merging area, thereby validating the model's effectiveness. (2) CAV Benefits: The safety grade improves progressively from Grade D to Grade A as the CAV penetration rate increases. (3) Performance Threshold: A critical improvement in safety grade (to Grade B) is achieved when the penetration rate reaches 30%; once it exceeds 40%, all evaluation indicators enter the "Excellent" range.

Table 12. Safety evaluation results under different CAV penetration rates.

Evaluation Indicators	0% (Baseline)	10%	20%	30%	40%	50%
K_1	1276 (C)	1089 (C)	852 (B)	740 (B)	482 (B)	266 (A)
K_2	0.46 (D)	0.392 (D)	0.307 (B)	0.267 (B)	0.174 (B)	0.096 (A)
K_3	178.223 (D)	142.647 (C)	113.562 (C)	96.237 (B)	69.316 (A)	42.557 (A)
K_4	55.25 (D)	49.63 (C)	41.247 (C)	28.639 (B)	18.726 (A)	10.244 (A)
Comprehensive evaluation	Grade D (Poor)	Grade C (Fair)	Grade C (Fair)	Grade B (Good)	Grade A (Excellent)	Grade A (Excellent)

5.2. Comparative Analysis and Contextualization of Findings

To meaningfully situate the contributions of this study within the existing body of knowledge, this section provides a comparative analysis. While direct quantitative comparison of absolute metrics (e.g., conflict counts) with prior studies is constrained by differences in data sources (high-fidelity simulation calibrated with a unique trajectory dataset) and analytical focus, a substantive discussion of perspectives, mechanisms, and methodologies is both possible and necessary.

(1) A robust consensus in the literature confirms that CAVs can enhance traffic safety, typically demonstrated through reductions in aggregate conflict frequency, surrogate safety indicators, or network-wide delays as penetration rates increase. Our findings corroborate this overarching trend, as evidenced by the comprehensive safety grade improvement (from D to A) in our case study. However, our framework advances the discourse by revealing the mechanism behind this improvement. The identification of a distinct spatial migration of high-risk zones—from the "static geometric bottleneck" at the merge point to a "dynamic interaction interface" on the mainline—provides a novel, granular explanation. This indicates that safety gains are achieved not through a uniform dampening of risk, but through a fundamental reconfiguration of traffic interactions and the spatial transfer of residual risk. This insight into the spatiotemporal evolution of risk addresses a gap in mechanistic interpretations of CAV impacts, complementing the macro-level trends well-established in the literature.

(2) Our proposed "prediction-location-evaluation "framework differs methodologically from common approaches. Many previous assessments rely either on retrospective analysis of historical accident data (ill-suited for emerging mixed traffic) or on outputs from computationally intensive microscopic simulations analyzed via aggregated KPIs. In contrast, our integration of a parsimonious statistical prediction model (Negative Binomial regression) with a lightweight, grid-based spatial mapping technique offers a unique balance. It maintains interpretability and computational efficiency while enabling high-resolution spatial diagnosis—a capability not typically combined in existing tools. The validation of our framework's baseline output (0% CAV scenario) against the known condi-

tions of the real-world case study (see Section 4.2.3) further strengthens the credibility of its scenario-based comparative analyses.

(3) Traditional safety evaluations often rely on one or a few key performance indicators, such as Time to Collision (TTC) or post-encroachment time (PET). Our study establishes a multi-dimensional evaluation system that integrates conflict frequency, density, composite risk, and crucially, spatial dispersion metrics. The synthesis of these dimensions through grey variable-weight clustering into a single safety grade (A–D) represents a shift towards holistic assessment. This approach provides a more operationally actionable output—a clear "safety health index" for the merging area—compared to presenting a list of separate metric values. The derived grade thresholds (Table 11) translate analytical findings into a practical diagnostic tool, directly addressing a need for clearer decision-support outputs in proactive safety management.

In summary, this comparative analysis highlights that our core contributions are complementary and advanced: we provide a spatiotemporal mechanism for known safety trends, introduce a validated hybrid methodology for efficient spatial diagnosis, and deliver a synthesized grading system for actionable assessment, thereby addressing identified gaps in the proactive safety management of mixed-traffic environments.

5.3. Synthesis of Core Findings and Management Implications

Building on the contextual analysis above, this study converges on three fundamental characteristics of safety in merging areas under mixed CAV traffic, with direct implications for management and design.

5.3.1. Core Findings

(1) The relationship between CAV penetration rate and safety is not linear but exhibits a key threshold effect. Analysis indicates a critical range around 30–40% penetration. Once exceeded, cooperative driving behaviors begin to dominate the traffic flow, triggering a nonlinear leap in the overall safety level. Below this threshold, the benefits are incremental and more susceptible to degradation by high traffic demand.

(2) The most critical safety vulnerability undergoes a systematic spatial shift. In low-CAV environments, risk is concentrated at the traditional "static geometric bottleneck" of the merging zone. As CAV penetration increases, the primary risk migrates to the "dynamic interaction interface" within the mainline lanes (particularly Lane 3), where platoons of CAVs and human-driven vehicles engage in sustained parallel travel. This finding necessitates a paradigm shift in safety management focus—from facility-based "spot management" of the merge point to traffic-stream-based "corridor management" of the mainline.

(3) The safety benefits of CAVs are not realized in isolation but are significantly modulated by underlying traffic conditions. High traffic volume (Q) or a high merging ratio (CR) can substantially attenuate the positive effects of CAVs. This indicates that achieving optimal safety requires synergistic optimization at the system level, considering the interaction between CAV penetration, demand management, and geometric design.

5.3.2. Management Implications and Application Directions

Based on the core findings of this study, we propose the following three management insights and application directions, aiming to provide a theoretical basis and practical pathways for the precise management and system optimization of freeway merging areas under mixed traffic conditions.

(1) Management measures should be differentiated according to the stages of CAV penetration. In the low penetration phase (<30%), the focus should be on conventional engineering optimizations, including ensuring an acceleration lane length of at least 220 m,

implementing coordinated ramp metering, and optimizing the geometric alignment of the merging area to mitigate static bottleneck risks dominated by human-driven vehicles. Upon entering the medium-to-high penetration phase ($\geq$30%), the management paradigm must shift from "facility governance" to "flow-state governance." The core objective becomes enhancing vehicle-infrastructure coordination capabilities, and monitoring/management resources should be reallocated to prioritize the dynamic interaction zones on the mainline lanes (especially Lane 3), enabling a precise response to risk migration.

(2) It is recommended to leverage the conflict prediction and spatial risk mapping models developed in this study to establish a dynamic safety situation awareness and early-warning system that integrates real-time CAV penetration rates with traffic flow data. This system would facilitate a transition from passive response to proactive intervention. By predicting the migration of risk hotspots, it can support the implementation of anticipatory measures such as lane-level speed guidance, variable speed limits, or cooperative lane-changing suggestions, thereby proactively smoothing traffic flow and resolving potential conflicts.

(3) Future revisions of road design standards and guidelines must proactively incorporate the characteristics of mixed traffic flow. This requires reserving necessary communication interfaces, data exchange protocols, and physical space (e.g., space for dedicated communication facilities, layouts for lanes and roadside units supporting cooperative control) at the infrastructure level to accommodate cooperative driving. This provides fundamental support at the regulatory and hardware levels for unlocking the full safety potential of intelligent transportation systems.

6. Conclusions

This study developed an integrated spatiotemporal safety assessment framework to address the safety evaluation challenges in freeway merging areas under mixed CAV and human-driven traffic. The main conclusions are as follows:

(1) A novel "prediction-location-evaluation" framework was proposed and validated, which bridges quantifiable conflict prediction with high-resolution, spatially explicit risk mapping. This approach overcomes the limitations of conventional methods regarding data dependency and coarse granularity.

(2) The framework reveals a fundamental shift in risk patterns with increasing CAV penetration: high-risk areas migrate systematically from the "static geometric bottleneck" at the ramp merge point to a "dynamic interaction interface" on the mainline. This spatial reconfiguration provides a mechanistic explanation for how CAVs enhance safety.

(3) A multi-dimensional safety evaluation system was established, integrating conflict frequency, severity, and spatial distribution. By applying grey variable-weight clustering, an objective safety grading system (A–D) was created. A case study demonstrated that increasing CAV penetration from 10% to 50% can improve the safety grade from D (Poor) to A (Excellent), offering a direct tool for quantifying CAV benefits.

(4) The study provides a complete methodological toolbox that includes models, indicators, and evaluation criteria, thereby supporting risk diagnosis, safety assessment, and informed decision-making for merging area management during the mixed-traffic transition.

Future work will focus on validating the framework with real-world connected vehicle data, extending it to more complex scenarios (e.g., urban weaving areas), and developing proactive intervention strategies based on the predicted risk patterns, thereby closing the loop from safety assessment to active prevention and control.

https://doi.org/10.3390/sym18050831

Author Contributions: Conceptualization, X.C.; methodology, Q.L.; software, X.G.; validation, X.C. and G.L.; formal analysis, G.L.; investigation, X.G.; resources, Y.J.; data curation, L.Y.; writing—original draft preparation, Q.L. and L.Y.; writing—review and editing, Y.J.; visualization, Q.L.; supervision, L.Y.; project administration, X.C.; funding acquisition, Y.J. All authors have read and agreed to the published version of the manuscript.

Funding: This research was funded by the Guangdong Basic and Applied Basic Research (Grant No. 2026A1515010260) and Intelligent Policing Key Laboratory of Sichuan Province (Grant No. ZNJW2025KFQN006).

Data Availability Statement: Data will be made available upon request.

Acknowledgments: The authors would like to thank the National Social Science Fund of China (Grant No. 25BGL225).

Conflicts of Interest: The authors declare no conflicts of interest.

References

1. Wang, W.Z.; Cheng, G.Z.; Wang, G.P. Modeling and simulation of heterogeneous traffic flow in urban expressway merging areas. *Int. J. Mod. Phys. C* **2026**, *37*, 2550153. [CrossRef]
2. Zheng, L.; Ismail, K.; Meng, X. Traffic conflict techniques for road safety analysis: Open questions and some insights. *Can. J. Civ. Eng.* **2014**, *41*, 633–641. [CrossRef]
3. Luo, Q.; Wang, H.H.; Yang, J.H.; Zang, X.D.; Chen, X.Q.; Postolache, O. Study on a multi-factor lane-changing risk resilience assessment model based on genetic algorithm and fault tree analysis. *Accid. Anal. Prev.* **2026**, *230*, 108443. [CrossRef]
4. Ma, Y.T.; Liu, Q.; Fu, J.; Liufu, K.M.; Li, Q. Collision-avoidance lane change control method for enhancing safety for connected vehicle platoon in mixed traffic environment. *Accid. Anal. Prev.* **2023**, *184*, 106999. [CrossRef]
5. Tomás, R.F.; Fernandes, P.; Macedo, E.; Bandeira, J.M.; Coelho, M.C. Assessing the emission impacts of autonomous vehicles on metropolitan freeways. *Transp. Res. Procedia* **2020**, *47*, 617–624. [CrossRef]
6. Raju, N.; Arkatkar, S.; Easa, S.; Joshi, G. Customizing the following behavior models to mimic the weak lane based mixed traffic conditions. *Transp. B Transp. Dyn.* **2022**, *10*, 20–47. [CrossRef]
7. Song, L.; Fan, W. Intersection capacity adjustments considering different market penetration rates of connected and automated vehicles. *Transp. Plann. Technol.* **2023**, *46*, 286–303. [CrossRef]
8. Guo, Y.; Ma, J.Q.; Leslie, E.; Huang, Z.T. Evaluating the effectiveness of integrated connected automated vehicle applications applied to freeway managed lanes. *IEEE Trans. Intell. Transp. Syst.* **2022**, *23*, 522–536. [CrossRef]
9. Ma, K.; Wang, H. How Connected and Automated Vehicle-Exclusive Lanes Affect On-Ramp Junctions. *J. Transp. Eng. Part. A-Syst.* **2021**, *147*, 04020157. [CrossRef]
10. Hu, X.; Zheng, Z.; Chen, D.; Sun, J. Autonomous vehicle's impact on traffic: Empirical evidence from waymo open dataset and implications from modelling. *IEEE Trans. Intell. Transp. Syst.* **2023**, *24*, 6711–6724. [CrossRef]
11. Yao, Z.H.; Wu, Y.M.; Wang, J.R.; Wang, Y.; Li, G.; Jiang, Y.S. Analyzing the impact of different lane management strategies on mixed traffic flow with CAV platoons. *Systems* **2026**, *14*, 55. [CrossRef]
12. Chen, X.Q.; Wu, S.B.; Shi, C.J.; Huang, Y.G.; Yang, Y.S.; Ke, R.M.; Zhao, J.S. Sensing Data Supported Traffic Flow Prediction via Denoising Schemes and ANN: A Comparison. *IEEE Sens. J.* **2020**, *20*, 14317–14328. [CrossRef]
13. Park, N.; Park, J.; Joo, Y.; Abdel-Aty, M. Micro-level hotspot identification at intersections using traffic conflict analysis. *Accid. Anal. Prev.* **2025**, *220*, 108167. [CrossRef] [PubMed]
14. Basso, F.; Muñoz, Y.; Pezoa, R.; Varas, M. Assessing factors influencing the occurrence of traffic conflicts: A vehicle-by-vehicle approach. *Transp. B Transp. Dyn.* **2024**, *12*, 2332716. [CrossRef]
15. Kamel, A.; Sayed, T.; Kamel, M. Real-time combined safety-mobility assessment using self-driving vehicles collected data. *Accid. Anal. Prev.* **2024**, *199*, 107513. [CrossRef]
16. Wang, C.; Xu, C.C.; Xia, J.X.; Qian, Z.D.; Lu, L.J. A combined use of microscopic traffic simulation and extreme value methods for traffic safety evaluation. *Transp. Res. Part C Emerg. Technol.* **2018**, *90*, 281–291. [CrossRef]
17. Ali, Y.; Haque, M.M.; Mannering, F. Assessing traffic conflict/crash relationships with extreme value theory: Recent developments and future directions for connected and autonomous vehicle and highway safety research. *Anal. Methods Accid. Res.* **2023**, *39*, 100276. [CrossRef]
18. Spahana, A.; Perumal, V. Spatiotemporal variation of traffic conflict at signalized intersections under non-lane-based traffic condition. *Transp. Res. Rec.* **2022**, *2677*, 326–340. [CrossRef]

19. Reza, I.; Haq, M.T.; Ksaibati, K. Identifying snowplow truck crash hotspots and spatial analysis of crashes in the mountainous roadways. *Int. J. Crashworthiness* **2025**, *30*, 23–35. [CrossRef]
20. Duan, Y.Z.; Shao, Q.; Lin, Z.P.; Wang, Y.L.; Bai, Q.W. A comprehensive double index left-turn conflict model at contraflow left-turn lane intersections. *Promet-Traffic Transp.* **2024**, *36*, 1054–1067. [CrossRef]
21. Grigonis, V.; Placiakis, J. A methodological approach to identifying unsafe intersections for micromobility users: A case study of Vilnius. *Sustainability* **2025**, *17*, 11053. [CrossRef]
22. Chen, X.Q.; Zhang, Z.H.; Li, Z.B.; Han, B.; Zheng, Y.W.; Biancardo, S.A. Microscopic aggregated traffic parameter extraction against complex camera motion interference. *Transp. Saf. Environ.* **2025**, *7*, tdaf056. [CrossRef]
23. Tian, Y.; Zhang, Z.; Li, Z.; Fu, X.; Wang, G.; Ma, Y.; Wu, J. Traffic conflict identification and risk assessment at ramp merging areas based on improved XGBoost and SHAP. *J. Transp. Eng. Part A Syst.* **2025**, *151*, 04025091. [CrossRef]
24. Lyngdoh, G.K. A novel approach for safety assessment at unsignalized intersections: Integrating spatial metrics into postencroachment time analysis under heterogeneous traffic conditions. *Traffic Inj. Prev.* **2025**, *26*, 482–489. [CrossRef] [PubMed]
25. Nasr, H.A.; Jin, J.L.; Huang, H.L.; Eljailany, H.A. Real-time risk identification of rear-end conflicts at unsignalized intersections. *Systems* **2025**, *13*, 827. [CrossRef]
26. Zhang, H.; Hou, N.H.; Zhang, J.H.; Li, X.Y.; Huang, Y. Evaluating the safety impact of connected and autonomous vehicles with lane management on freeway crash hotspots using the surrogate safety assessment model. *J. Adv. Transp.* **2021**, *2021*, 5565343. [CrossRef]
27. Guo, Y.Y.; Liu, P.; Wu, Y.; Li, Q. Safety evaluation of unconventional signalized intersections based on conflict extreme value model. *China J. Highw. Transp.* **2022**, *35*, 85–92.
28. Abdel-Aty, M.; Wang, Z.J.; Zheng, O.; Abdelraouf, A. Advances and applications of computer vision techniques in vehicle trajectory generation and surrogate traffic safety indicators. *Accid. Anal. Prev.* **2023**, *191*, 107191. [CrossRef]
29. Faden, A.; Abdel-Aty, M.; Hasan, T.; Rim, H. Time-based safety performance functions of metered ramps and merge sections. *J. Transp. Eng. Part A Syst.* **2025**, *151*, 04025007. [CrossRef]
30. Kumar, A.; Mudgal, A. Risk assessment of rear-end crashes by incorporating vehicular heterogeneity into bayesian hierarchical extreme value models. *Transp. B Transp. Dyn.* **2024**, *12*, 2323058. [CrossRef]
31. Lyu, N.C.; Wang, Y.G.; Zhou, Y.; Wu, C.Z. Review of road traffic safety analysis and evaluation methods. *China J. Highw. Transp.* **2023**, *36*, 183–201.
32. Faden, A.; Abdel-Aty, M.; Mahmoud, N.; Hasan, T.; Rim, H. Multivariate Poisson-lognormal models for predicting peak-period crash frequency of joint on-ramp and merge segments on freeways. *Transp. Res. Rec.* **2024**, *2678*, 133–147. [CrossRef]
33. Zhang, Y.X.; Wang, C.; Yu, R.L.; Wang, L.Y.; Quan, W.; Gao, Y.; Li, P.F. The AD4CHE Dataset and Its Application in Typical Congestion Scenarios of Traffic Jam Pilot Systems. *IEEE Trans. Intell. Veh.* **2023**, *8*, 3312–3323. [CrossRef]
34. Tarko, A.P. A Unifying View on Traffic Conflicts and Their Connection with Crashes. *Accid. Anal. Prev.* **2021**, *158*, 106187. [CrossRef] [PubMed]
35. Fu, C.Y.; Lu, Z.Y.; Ding, N.K.; Bai, W. Distance headway-based safety evaluation of emerging mixed traffic flow under snowy weather. *Phys. A* **2024**, *642*, 129792. [CrossRef]
36. Zhu, S.Y.; Jiang, R.X.; Wang, H.; Zou, H.; Wang, P.; Qiu, J. A review of motor vehicle traffic conflict techniques. *China J. Highw. Transp.* **2020**, *33*, 15–33.
37. Yang, Y.; Huang, H.B.; Li, G.; Han, B.R.; Yuan, Z.Z.; Ma, H. A systematic review of resilience assessment and enhancement of urban integrated transportation networks. *J. Transp. Geogr.* **2025**, *129*, 104420. [CrossRef]
38. Chen, G. Research on the Spatial Distribution Characteristics of Traffic Conflicts in the Weaving Area of Expressway. Master's thesis, Southeast University, Nanjing, China, 2023.
39. Luo, Q.; Lu, X.; Zang, Z.J.; Gong, H.W.; Guo, X.Y.; Chen, X.Q. A real-time early warning framework for multi-dimensional driving risk of heavy-duty trucks using trajectory data. *Systems* **2026**, *14*, 204. [CrossRef]
40. Talavera, E.; Díaz-Álvarez, A.; Jiménez, F.; Naranjo, J.E. Impact on Congestion and Fuel Consumption of a Cooperative Adaptive Cruise Control System with Lane-Level Position Estimation. *Energies* **2018**, *11*, 194. [CrossRef]
41. Yan, X.H.; Lu, D.; Liu, T.; Zhang, B. Evaluation of recycled aggregate based on analysis hierarchy process-grey variable weight clustering. *Adv. Concr. Constr.* **2024**, *18*, 205–211.
42. Li, G.; Ji, S.X.; Cheng, W.R.; Wang, W.Y.; Yan, X.Y.C.; Yang, Z.; Zhang, J. A new framework for modelling traffic conflict interval time based on correlated random parameter duration model with heterogeneity in means and variances. *Accid. Anal. Prev.* **2026**, *224*, 108282. [CrossRef]

Disclaimer/Publisher's Note: The statements, opinions and data contained in all publications are solely those of the individual author(s) and contributor(s) and not of MDPI and/or the editor(s). MDPI and/or the editor(s) disclaim responsibility for any injury to people or property resulting from any ideas, methods, instructions or products referred to in the content.